IN VIVO *39*: 749-757 (2025)
doi: 10.21873/invivo.13879

Boron-dipyrromethene Staining May Enhance Fat Detection in the MASLD Zebrafish Model: NGS-validated lncRNA Profiling

WOOKJAE JUNG[1], MIN HYE KIM[1], JUNG WOOK YANG[1,2,3], DONG CHUL KIM[1,2,3], JONG SIL LEE[1,2,3], JEONG-HEE LEE[1,2,3], HYO JUNG AN[2,3,4*] and DAE HYUN SONG[2,3,4*]

[1]Department of Pathology, Gyeongsang National University Hospital, Jinju, Republic of Korea;
[2]Department of Pathology, Gyeongsang National University School of Medicine, Jinju, Republic of Korea;
[3]Institute of Medical Sciences, Gyeongsang National University, Jinju, Republic of Korea;
[4]Department of Pathology, Gyeongsang National University Changwon Hospital, Changwon, Republic of Korea

Abstract

Background/Aim: Metabolic dysfunction–associated steatotic liver disease (MASLD) is a serious global public health concern. Long non-coding RNAs (lncRNAs) have been identified as key contributors to MASLD pathogenesis. Zebrafish can be utilized to study the relationship between MASLD and lncRNAs because of their similarity to human genes. Oil Red O staining is a traditional method for confirming liver fatty changes; however, it has several limitations. This study aimed to evaluate the efficacy of boron-dipyrromethene (BODIPY) in detecting fatty changes in the liver.
Materials and Methods: Liver tissues were collected from 30 zebrafish that were fed a BODIPY-containing high-cholesterol diet. Oil Red O and BODIPY staining were evaluated by two pathologists, and next-generation sequencing (NGS) was performed using liver tissues categorized into high fatty change (six liver tissues) and low fatty change (six liver tissues) groups.
Results: BODIPY and Oil Red O staining of zebrafish liver sections correlated significantly (p=0.009). NGS identified eight differentially expressed lncRNAs with over a 10-fold difference between the high- and low-fatty acid change groups. Of these, three showed lncRNA-mRNA interaction networks linked to human disorders.
Conclusion: BODIPY staining is a reliable alternative to Oil Red O staining for assessing fatty changes in MASLD zebrafish models, particularly when examining frozen liver sections.

Keywords: Metabolic dysfunction–associated steatotic liver disease (MASLD), Boron-dipyrromethene (BODIPY), long non-coding RNA (lncRNA), zebrafish.

*These Authors contributed equally to this study.

Hyo Jung An, MD, Institute of Medical Science, Gyeongsang National University, Gyeongsang National University School of Medicine, 79 Gangnam-ro, Jinju 52727, Republic of Korea. Tel: +82 552143150, Fax: +82 552143174, e-mail: ariel2020@naver.com and Dae Hyun Song, MD, Institute of Medical Science, Gyeongsang National University, Gyeongsang National University School of Medicine, 79 Gangnam-ro, Jinju 52727, Republic of Korea. Tel: +82 552143152, Fax: +82 552143174, e-mail: golgy@hanmail.net

Received November 29, 2024 | Revised December 14, 2024 | Accepted December 16, 2024

Introduction

Metabolic dysfunction–associated steatotic liver disease (MASLD), previously named nonalcoholic fatty liver disease (NAFLD), refers to a group of related liver disorders, including metabolic dysfunction-associated steatohepatitis (MASH), cirrhosis, and hepatocellular carcinoma (1, 2). MASLD is the most common cause of chronic liver disease, with a 25% global prevalence, and is the leading cause of liver-related morbidity and mortality. Thus, a deep understanding of the pathophysiological mechanisms driving MASLD is essential for developing targeted therapies (3). Owing to its nature as a multisystem disease that is associated with insulin resistance, oxidative stress, the cell death pathway, and adipocytokines, elucidating the pathophysiological mechanisms of MASLD remains challenging (4).

Non-coding RNAs, particularly long non-coding RNA (lncRNAs; non-coding transcripts of over 200 nucleotides), are associated with various metabolic disorders (5). In addition, lncRNAs are involved in various physiological processes, including cell differentiation and developmental regulation, cytokine expression, endotoxic shock, inflammatory and neuropathic pain, cholesterol biosynthesis and homeostasis, glucose metabolism, cell signaling, and transport pathways (6). lncRNAs are important genetic factors involved in MASLD-associated fibrosis (7).

Zebrafish are freshwater fish belonging to the minnow family. In the 1930s, zebrafish were first used as a research model, owing to their short reproduction period (three to four months) (8). In addition, because of their genetic similarity to humans, transparent embryos, and applicability in large-scale screening, zebrafish have emerged as a valuable model organism in biomedical research (9). The zebrafish has emerged as a useful model for investigating MASLD for the following reasons: zebrafish genes can be easily manipulated; the zebrafish MASLD model is physiologically similar to MASLD in humans; and fatty liver and lipid absorption processes are easily observable in tissues using oil red O staining and fluorescently labeled fatty acid analogs, respectively (10).

Oil Red O staining is frequently used to visualize fat droplets; however, it is associated with several limitations. For example, it forms precipitates and red crystals that affect the interpretation of the results (11). Fluorescence imaging is a convenient method for visualizing the dynamics of lipid droplets in a cellular environment. Boron–dipyrromethene (BODIPY) is a fluorescent dye with high specificity and sensitivity, more accurately representing fatty acid accumulation and distribution (12). Liver tissue BODIPY staining and hepatic steatosis assessment have been successfully conducted in a rat model using fluorescent-stained lipid droplet analysis (13). In addition, Miyares *et al.* showed that BODIPY-labeled fatty acids can be delivered to zebrafish yolks to visualize lipid and lipoprotein dynamics and measure fatty acid metabolism (14).

In this study, we hypothesized that immunofluorescence microscopy with BODIPY dye is superior to optical microscopy with Oil Red O staining in evaluating fatty acid accumulation and distribution in the livers of zebrafish fed a high-cholesterol diet. Therefore, in this study, we aimed to determine the sensitivity and specificity of immuno-fluorescence microscopy with BODIPY dye in evaluating fatty acid accumulation and distribution in the livers of zebrafish fed a high-cholesterol diet and compare it with that of optical microscopy with Oil Red O staining. In addition, we aimed to identify lncRNAs involved in the development of MASLD in the zebrafish model using next-generation sequencing (NGS).

Materials and Methods

The high cholesterol diet fed adult zebrafish model. Thirty wild-type AB line adult zebrafish (3 months post-fertilization) were included in the experiment. The zebrafish were kept in a water tank that was maintained at 28˚C. A high-cholesterol diet was prepared as previously described by Kan Chen *et al.* (15) using gemma micro (ZF 300, Skretting, Tooele, UT, USA) as the basic food. Cholesteryl BODIPY 542/563 C11 was dissolved in chloroform and mixed with the food. Following complete chloroform evaporation, the food contained the fluorescent probe

[1/100,000 (w/w)]. All 30 zebrafish were fed the resulting food [a high-cholesterol diet (1.5 g per day)] for eight weeks.

Eight weeks later, the zebrafish were anesthetized with 10 g of ethyl3-aminobenzoate methanesulfonate (#E10521, Sigma, Burlington, MA, USA) for 3-5 min and euthanized. This study was approved by the Institutional Animal Care and Use Committee of the Gyeongsang National University (GNU-240710-E0140). All experiments involving live animals were performed in accordance with the relevant guidelines and regulations and are reported in accordance with the ARRIVE guidelines.

Evaluation of fatty changes in the liver. For staining, the frozen tissues of each zebrafish were cut longitudinally into 4-μm thick sections. Eight or more frozen liver sections were obtained from each zebrafish; six or more were stained with Oil Red O as described in our previous study (16), one was stained with hematoxylin and eosin (H&E), and the remaining one was used for fluorescence microscopy examination.

Propylene glycol (80%) was added for 2 min, and Oil Red O staining was performed for 35 min. After washing the stained slides twice with distilled water, microscopic washing was performed to prevent overstaining. This method was identical to that used in our previous study (16). The proportion of fatty changes on each slide stained with Oil Red O was blindly evaluated by two pathologists. The value of the section with the highest true signal proportion after oil red O staining was used as the representative value. BODIPY liver samples were observed by immunofluorescence microscopy using a fluorescein isothiocyanate (FITC) filter (UV light intensity, ND4 filter, and exposure time of 300 ms). BODIPY staining was categorized into three classes (1+, 2+, and 3+) according to the immunofluorescence reading criteria on human kidney biopsy and was interpreted by two pathologists.

RNA extraction and next-generation sequencing analysis. A scalpel was used to obtain liver tissue from the remaining frozen specimens. The tissue was immediately crushed in 10 μl of Trizol (#15596026, Invitrogen, Carlsbad, CA, USA) and stored at −70˚C. Based on the fatty change measurements of the liver tissue, six zebrafish samples were assigned to the low- and high-fatty liver groups. Six specimens with a BODIPY score of 1+ and an oil red O score of 0% were included in the low group, whereas six specimens with BODIPY scores of 3+ or 2+ with a high oil red O score (20-30%) were included the high group. Liver specimens of zebrafish numbers 1, 9, 19, 21, 22, and 25 with high fatty liver scores based on oil red O staining and BODIPY were pooled into a "high" group. Zebrafish numbers 3, 4, 6, 10, 15, and 18 were pooled into a "low" group. RNA was extracted from the two pooled groups. The method of RNA extraction from the tissue is described in our previous study (16). Total RNA was depleted of rRNA using the Ribo-zero H/M/R Gold kit (Illumina, San Diego, CA, USA), according to the manufacturer's instructions. Library preparation and quality validation were conducted prior to NGS. Total RNA integrity was assessed using an Agilent Technologies 2100 Bioanalyser (Agilent, Santa Clara, CA, USA), ensuring an RNA Integrity Number (RIN) of seven or higher. To confirm the size of the PCR-enriched fragments, we evaluated the template size distribution using an Agilent Technologies 2100 Bioanalyzer equipped with a DNA 1000 chip. Transcriptome sequencing was performed on an Illumina platform, and raw sequencing data were quantified as fragments per kilobase of exons per million fragments mapped (FPKM) for each sample. The statistical significance of the fold changes in the transcript expression profiles was analyzed using paired t-tests (Macrogen, Seoul, Republic of Korea).

Results

BODIPY was superior to oil red O staining in the liver specimens of the zebrafish. The fatty liver change scores of 30 adult zebrafish after 8 weeks of high-cholesterol diet consumption are summarized in Table I. Eight frozen liver sections were obtained from zebrafish 25. The frozen section stained with H&E revealed no observable changes in fat content. It was difficult to identify the lipid droplets because they were dissolved in the organic solvent used during the H&E staining process, leaving only an empty space (Figure 1A). Another frozen liver section (from the same sample, zebrafish 25) was used for immunofluorescence microscopy. A diffuse positive signal for BODIPY was detected using immunofluorescence (Figure 1B). The remaining six frozen sections were used for the oil red O staining; partially positive red droplets were observed at the center of the image (Figure 1C). The highest observed among the six slides was considered the representative value. Oil-red O staining sections were difficult to interpret because of tissue detachment during washing with distilled water (Figure 1C). A statistically significant correlation was observed between the BODIPY and Oil Red O scores (p=0.009, linear-by-linear association).

Identification of long noncoding RNAs associated with nonalcoholic fatty liver disease in zebrafish. After library preparation and validation quality checks, the high- and low-fatty liver groups were included in the final RNA sequencing. Using NGS, differentially expressed gene (DEG) analyses were performed between high and low fatty change groups using edgeR; 5065 DEGs (genes that satisfied the |fold change| ≥2 and p-value <0.05 conditions) were identified. Among the 5,065 genes, 1,772 were significantly up-regulated and, 3,293 were significantly down-regulated. We selected eight lncRNAs (ZFLNCT14973, ZFLNCT11502, ZFLNCT03767, ZFLNCT08104, ZFLNCT11854, ZFLNC T00315, ZFLNCT18769, and ZFLNCT04118) with greater than ten-fold changes (Table II).

Discovery of human homologs for the eight long noncoding RNAs identified in zebrafish. Human homologs of these eight lncRNAs according to ZFLNC are ENST00000475761, ENST00000474557, NONHSAT075167, NONHSAT188126, ENST00000555934, ENST00000415070, ENST000005 87701, NONHSAT180080, and NONHSAT174445 (Table II). We searched for these human loci in the Ensembl (17-21) and NONCODE (22-25) databases to obtain general information, sequences, expression profiles in human tissues, and exosome expression profiles.

Table I. *Boron-dipyrromethene (BODIPY) score compared with oil-red O stain in liver specimen of the zebrafish.*

No.	BODIPY score in liver	Oil red O stain in liver	NGS group
1	3+	NI	H
2	1+	0%	
3	1+	0%	L
4	1+	0%	L
5	2+	10%	
6	1+	0%	L
7	2+	5%	
8	1+	10%	
9	2+	30%	H
10	1+	0%	L
11	2+	5%	
12	1+	5%	
13	1+	5%	
14	2+	10%	
15	1+	0%	L
16	1+	2%	
17	2+	15%	
18	1+	0%	L
19	2+	30%	H
20	1+	5%	
21	2+	20%	H
22	2+	20%	H
23	2+	10%	
24	1+	2%	
25	3+	15%	H
26	1+	15%	
27	1+	10%	
28	1+	20%	
29	1+	5%	
30	1+	5%	

BODIPY liver samples were observed by immunofluorescence microscopy using a fluorescein isothiocyanate (FITC) filter (UV light intensity, ND4 filter, and exposure time 300 ms), Oil-Red O staining was performed on six or more sections, and the value of the section with the highest true signal proportion after staining was taken as the representative value. NI: Not informative, due to tissue loss; NGS: next-generation sequencing (RNA-seq); H: high group pooled; L: low group pooled (p-value=0.009 by linear association).

Using the Zebrafish LncRNA Database (26-28), we confirmed that there is a lncRNA-mRNA (protein-coding gene) interaction network between four of the eight lncRNAs in zebrafish, three of which (ZFLNCT11854, ZFLNCT00315, and ZFLNCT18769) (LOC100537717, b3gat2, dnm1b, nlgn3b, s100a1, trpm4c, and zgc:100864) are associated with human diseases, including type 2 diabetes mellitus, Barrett's esophagus, schizophrenia,

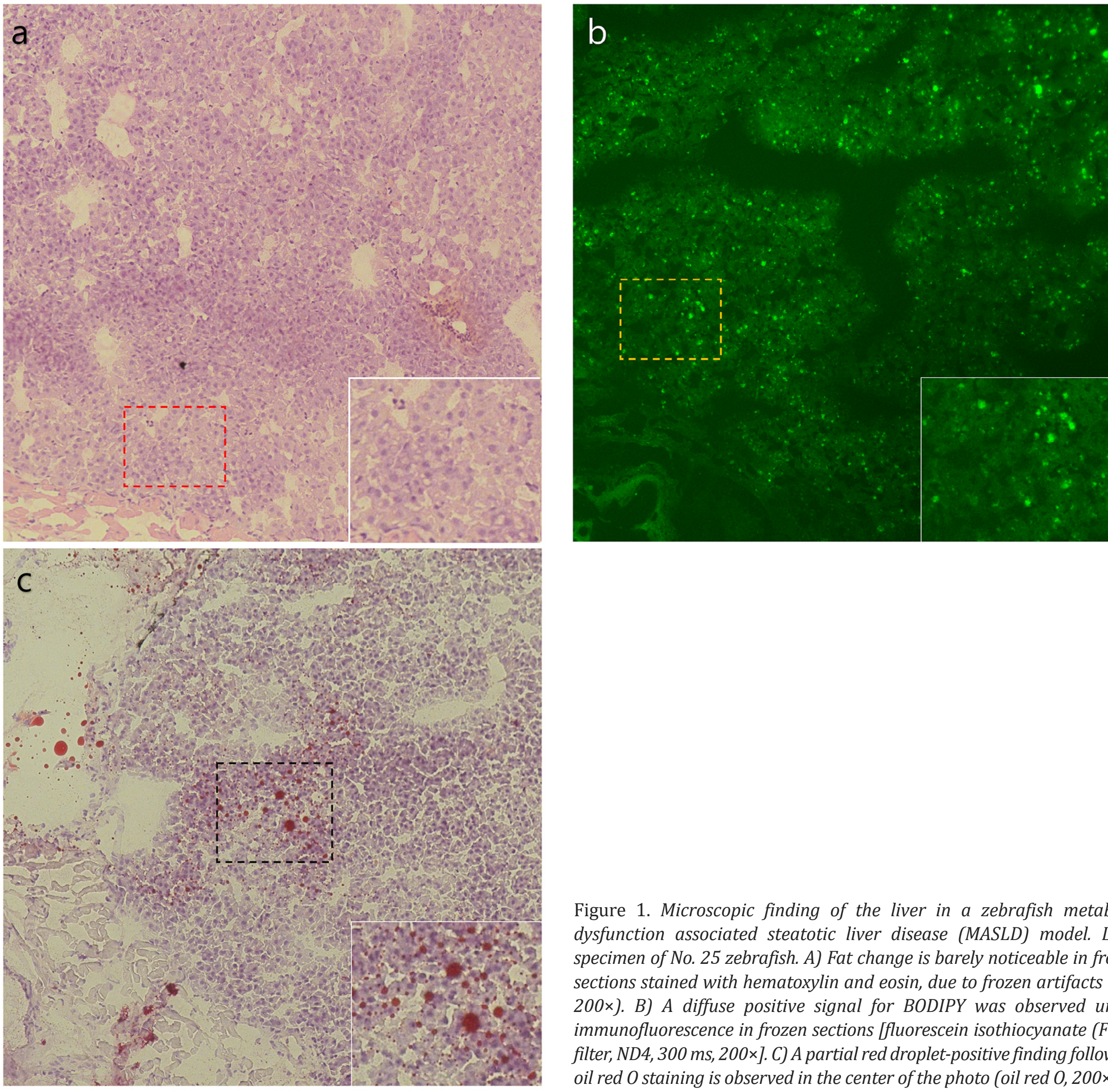

Figure 1. *Microscopic finding of the liver in a zebrafish metabolic dysfunction associated steatotic liver disease (MASLD) model. Liver specimen of No. 25 zebrafish. A) Fat change is barely noticeable in frozen sections stained with hematoxylin and eosin, due to frozen artifacts (HE, 200×). B) A diffuse positive signal for BODIPY was observed under immunofluorescence in frozen sections [fluorescein isothiocyanate (FITC) filter, ND4, 300 ms, 200×]. C) A partial red droplet-positive finding following oil red O staining is observed in the center of the photo (oil red O, 200×).*

developmental and epileptic encephalopathy, autistic disorders, cardiomyopathies, erythrokeratodermia variabilis, progressive familial heart block type IB, and leukocyte adhesion deficiency type II (Table III).

ZFLNCT14973 was one of the down-regulated lncRNAs identified in our previous study (16). We searched the Ensembl database for human homologs of ZFLNCT14973, ENST00000475761, and ENST00000405276. Among them, ENST00000405276 is the transcript of YWHAZP10-201, which is a processed pseudogene transcribed from ENSG00000217624 (YWHAZP10) (29). YWHAZP10 is associated with hyperammonemia and X-linked intellectual disability (30). In addition, YWHAZP10 is expressed in synovial

Table II. *Eight potential metabolic dysfunction–associated steatotic liver disease-associated lncRNAs.*

NCBI transcript ID	ZFLNC ID	Human homology by ZFLNC	H/L FC	H/L p-Value
XR_002458928	ZFLNCT14973	ENST00000475761; ENST00000405276;	–71.6932546059851	2.42384873032383E-18
XR_662216	ZFLNCT11502	ENST00000474557; NONHSAT092278;	–49.3767654066024	4.59696546299878E-22
XR_001798259, XR_002458163, XR_002458164, XR_002458165, XR_223487	ZFLNCT03767	NONHSAT075167;	–38.2973723605676	1.22006069675629E-23
XR_001798627	ZFLNCT08104	NONHSAT188126;	–16.307178381604	0.000143700813095602
XR_222135, XR_663270, XR_663271	ZFLNCT11854	ENST00000555934; NR_015358; NONHSAT037289	–16.0138370641219	3.22931019466792E-28
NR_015622	ZFLNCT00315	ENST00000415070; NONHSAT182102;	–12.5048208637977	2.12865617865362E-47
XR_001798583	ZFLNCT18769	ENST00000587701; NONHSAT180080;	–12.2545386578688	0.00200946384535737
XR_002458426, XR_661044	ZFLNCT04118	NONHSAT174445;	–11.9948300966469	8.73388143763262E-18

Next generation sequencing (RNAseq) results showed 58 lncRNAs that differed by more than 10-fold between BODIPY low and high groups; eight candidates with confirmed human homology in the ZFLNC search. H/L: High group/low group; FC: fold change.

macrophages of patients with remissive rheumatoid arthritis and in juvenile idiopathic arthritis patients treated with lipopolysaccharide (LPS) (30). Currently, the association of this gene with MASLD is unknown; however, considering that this gene was down-regulated in both our previous and the present study, we cautiously hypothesize that this gene is associated with MASLD.

Discussion

As MASLD worsens, liver fibrosis plays an important role in its progression and associated complications and fibrosis progression may lead to the development of liver cancer and cardiovascular disease (31). MASLD treatment aims to improve inflammatory fibrosis of the liver and the treatment of concomitant metabolic diseases (obesity, diabetes, dyslipidemia, and hypertension) for the purpose of reducing the incidence or mortality of cardiovascular disease or cirrhotic liver cancer (32). Although new drugs are under development for MASLD, resmetirom is currently the only FDA-approved drug, and lifestyle modification remains the recommended treatment across all stages of MASH (33).

Oil-Red O staining has traditionally been used to confirm steatosis in zebrafish (34). However, Oil Red O staining is associated with several limitations. For example, the use of ethanol or isopropanol in Oil Red O staining often results in the destruction and fusion of lipid droplets (35). In addition, Oil Red O solution has a limited shelf life, requiring fresh powder dissolution and filtration, which can lead to inconsistent results (13). In addition, the Oil-Red O stains more than lipid droplets, leading to an overestimation of steatosis (36). To overcome these shortcomings, we quantified the degree of fatty changes in the liver using immunofluorescence microscopy with the fluorescent dye BODIPY. We then compared the BODIPY score, which quantifies the results using BODIPY dye, with the proportion of fatty changes determined using oil red O staining, and a significant correlation was found.

Table III. *lncRNA–mRNA (protein-coding gene) interaction network and related human disorder.*

ZFLNC ID	Correlated coding gene	Related human disorder
ZFLNCT11854	LOC100537717	Type 2 diabetes mellitus
	b3gat2	Barrett's esophagus
		Schizophrenia
	dnm1b	Developmental and epileptic encephalopathy 31A
		Developmental and epileptic encephalopathy 31B
	nlgn3b	Autistic disorder
ZFLNCT00315	s100a1	Cardiomyopathies
ZFLNCT18769	trpm4c	Erythrokeratodermia variabilis et progressiva 6
		Progressive familial heart block type IB
	zgc:100864	Leukocyte adhesion deficiency, type II

(ZFLNCT11854, ZFLNCT00315, and ZFLNCT18769) and (LOC100537717, b3gat2, dnm1b, nlgn3b, s100a1, trpm4c, and zgc:100864) are associated with human diseases, including type 2 diabetes mellitus, Barrett's esophagus, schizophrenia, developmental and epileptic encephalopathy, autistic disorders, cardiomyopathies, erythrokeratodermia variabilis, progressive familial heart block type IB, and leukocyte adhesion deficiency type II.

To the best of our knowledge, this is the first study to compare immunofluorescence microscopy with BODIPY dye and optical microscopy with Oil Red O staining. Consequently, it is the first study to confirm that immunofluorescence microscopy with BODIPY dye for fatty acid accumulation and distribution evaluation in the livers of zebrafish fed a high-cholesterol diet was superior to that of optical microscopy with Oil Red O staining. NGS technology has the advantage of high specificity and sensitivity, so it can detect genes with weak expression and can perform analysis on samples without a reference genome (37). Therefore, we identified DEGs in the high-fat diet-fed zebrafish using NGS. Comparing the identified DEGs (lncRNAs) to the lncRNAs found in our previous study revealed that ZFLNCT14973, which was down-regulated in the high fatty liver group, was also found to be down-regulated in our previous study (16). Although the pathophysiological function of this gene in MASLD is unknown, the confirmation of results indicates that BODIPY staining and Oil Red O staining led to the same finding; thus, BODIPY staining serves as an alternative to Oil Red O staining.

In addition, we identified eight lncRNAs whose expression levels differed by more than 10-fold between the high- and low-fatty liver groups. Each lncRNA was identified using the information provided by ZFLNC (26-28, 38). Among them, four (ZFLNCT03767, ZFLNCT11854, ZFLNCT00315, and ZFLNCT18769) had lncRNA-mRNA (protein-coding gene) interaction networks, and three (ZFLNCT11854, ZFLNCT00315, and ZFLNCT18769) were associated with human diseases (LOC100537717, b3gat2, dnm1b, nlgn3b, s100a1, trpm4c, and zgc:100864) including type 2 diabetes mellitus, Barrett's esophagus, schizophrenia, developmental and epileptic encepha-lopathy, autistic disorder, cardiomyopathies, erythrokeratodermia variabilis et progressive, progressive familial heart block type IB, and leukocyte adhesion deficiency, type II. In both our previous study and this study, we searched the Ensembl database for the human homologue of lncRNA ZFLNCT14973 (ENST00000475761, ENST00000405276), which was down-regulated in the high-fatty liver group. Of these, ENST00000405276 is the processed pseudogene transcript YWHAZP10-201, which is transcribed from ENSG00000 217624 (YWHAZP10). Literature search results suggest that YWHAZP10 is associated with hyperammonemia, X-linked electronic disability, rheumatoid arthritis, and juvenile idiopathic arthritis (30). Although the role of the gene in the pathophysiological mechanism of MASLD is unknown, the results suggest that YWHAZP10 is strongly associated with MASLD, and evaluating its interaction network may elucidate its role in MASLD.

In conclusion, BODIPY staining is effective in evaluating the degree of fatty liver changes in a zebrafish MASLD model and overcomes the limitations associated with Oil Red O staining. In addition, lncRNA data obtained from zebrafish samples classified by BODIPY staining are expected to increase our understanding of the pathophysiological mechanisms of MASLD and contribute to the development of treatment strategies.

Conflicts of Interest

The Authors declare that they have no conflicts of interest in relation to this study.

Authors' Contributions

WJ Jung: Project development, Data analysis, Manuscript writing; MH Kim: Data analysis; JW Yang: Manuscript editing, Data analysis; DC Kim: Data analysis; JS Lee: Data analysis; JH Lee: Data analysis; HJ An: Manuscript editing, Data analysis, Supervisor; DH Song: Manuscript editing, Data analysis, Supervisor.

Acknowledgements

This research was supported by the grant from Institute of Medical Science of Gyeongsang National University (IMS GNU-2023-02). This research was supported by Basic Science Research Program through the National Research Foundation of Korea (NRF) funded by the Ministry of Education (2020R1I1A30518661). This work was supported by the National Research Foundation of Korea (NRF) grant funded by the Korean government (MSIT) (RS-2022-00166664).

References

1 Cohen JC, Horton JD, Hobbs HH: Human fatty liver disease: old questions and new insights. Science 332(6037): 1519-1523, 2011. DOI: 10.1126/science.1204265
2 Rinella ME, Lazarus JV, Ratziu V, Francque SM, Sanyal AJ, Kanwal F, Romero D, Abdelmalek MF, Anstee QM, Arab JP, Arrese M, Bataller R, Beuers U, Boursier J, Bugianesi E, Byrne CD, Castro Narro GE, Chowdhury A, Cortez-Pinto H, Cryer DR, Cusi K, El-Kassas M, Klein S, Eskridge W, Fan J, Gawrieh S, Guy CD, Harrison SA, Kim SU, Koot BG, Korenjak M, Kowdley KV, Lacaille F, Loomba R, Mitchell-Thain R, Morgan TR, Powell EE, Roden M, Romero-Gómez M, Silva M, Singh SP, Sookoian SC, Spearman CW, Tiniakos D, Valenti L, Vos MB, Wong VW, Xanthakos S, Yilmaz Y, Younossi Z, Hobbs A, Villota-Rivas M, Newsome PN, NAFLD Nomenclature consensus group: A multisociety Delphi consensus statement on new fatty liver disease nomenclature. J Hepatol 79(6): 1542-1556, 2023. DOI: 10.1016/j.jhep.2023.06.003
3 Badmus OO, Hillhouse SA, Anderson CD, Hinds TD, Stec DE: Molecular mechanisms of metabolic associated fatty liver disease (MAFLD): functional analysis of lipid metabolism pathways. Clin Sci (Lond) 136(18): 1347-1366, 2022. DOI: 10.1042/CS20220572
4 Younossi ZM: Review article: current management of non-alcoholic fatty liver disease and non-alcoholic steatohepatitis. Aliment Pharmacol Ther 28(1): 2-12, 2008. DOI: 10.1111/j.1365-2036.2008.03710.x
5 Ji E, Kim C, Kim W, Lee EK: Role of long non-coding RNAs in metabolic control. Biochim Biophys Acta Gene Regul Mech 1863(4): 194348, 2020. DOI: 10.1016/j.bbagrm.2018.12.006
6 Mattick JS, Amaral PP, Carninci P, Carpenter S, Chang HY, Chen LL, Chen R, Dean C, Dinger ME, Fitzgerald KA, Gingeras TR, Guttman M, Hirose T, Huarte M, Johnson R, Kanduri C, Kapranov P, Lawrence JB, Lee JT, Mendell JT, Mercer TR, Moore KJ, Nakagawa S, Rinn JL, Spector DL, Ulitsky I, Wan Y, Wilusz JE, Wu M: Long non-coding RNAs: definitions, functions, challenges and recommendations. Nat Rev Mol Cell Biol 24(6): 430-447, 2023. DOI: 10.1038/s41580-022-00566-8
7 Hanson A, Wilhelmsen D, DiStefano JK: The role of long non-coding RNAs (lncRNAs) in the development and progression of fibrosis associated with nonalcoholic fatty liver disease (NAFLD). Noncoding RNA 4(3): 18, 2018. DOI: 10.3390/ncrna4030018
8 Zebrafish show their stripes. Lab Anim (NY) 41(9): 247, 2012. DOI: 10.1038/laban0912-247
9 Lieschke GJ, Currie PD: Animal models of human disease: zebrafish swim into view. Nat Rev Genet 8(5): 353-367, 2007. DOI: 10.1038/nrg2091
10 Seth A, Stemple DL, Barroso I: The emerging use of zebrafish to model metabolic disease. Dis Model Mech 6(5): 1080-1088, 2013. DOI: 10.1242/dmm.011346
11 Du J, Zhao L, Kang Q, He Y, Bi Y: An optimized method for Oil Red O staining with the salicylic acid ethanol solution. Adipocyte 12(1): 2179334, 2023. DOI: 10.1080/21623945.2023.2179334
12 Zhu J, Tan NK, Kikuchi K, Kaur A, New EJ: BODIPY-based fluorescent indicators for lipid droplets. Analysis Sensing 4(1): e202300049, 2024. DOI: 10.1002/anse.202300049
13 Garcia K, Alves A, Ribeiro-rodrigues TM, Reis F, Viana S: Analysis of fluorescent-stained lipid droplets with 3D reconstruction for hepatic steatosis assessment. J Vis Exp (196), 2023. DOI: 10.3791/65206
14 Miyares RL, de Rezende VB, Farber SA: Zebrafish yolk lipid processing: a tractable tool for the study of vertebrate lipid transport and metabolism. Dis Model Mech 7(7): 915-927, 2014. DOI: 10.1242/dmm.015800

15 Chen K, Wang CQ, Fan YQ, Xie YS, Yin ZF, Xu ZJ, Zhang HL, Cao JT, Han ZH, Wang Y, Song DQ: Optimizing methods for the study of intravascular lipid metabolism in zebrafish. Mol Med Rep 11(3): 1871-1876, 2015. DOI: 10.3892/mmr.2014.2895
16 An HJ, Lee YJ, Choe CP, Cho HK, Song DH: Long noncoding RNAs associated with nonalcoholic fatty liver disease in a high cholesterol diet adult zebrafish model. Sci Rep 11(1): 23005, 2021. DOI: 10.1038/s41598-021-02455-0
17 Transcript: ENST00000475761.3. Ensembl. Available at: https://www.ensembl.org/Homo_sapiens/Transcript/Summary?db=core;g=ENSG00000242559;r=X:41683168-41683462;t=ENST00000475761 [Last accessed on December 12, 2024]
18 Transcript: ENST00000474557.1. Ensembl. Available at: https://www.ensembl.org/Homo_sapiens/Transcript/Summary?db=core;g=ENSG00000244101;r=3:136609050-136609602;t=ENST00000474557 [Last accessed on December 12, 2024]
19 Transcript: ENST00000555934.1. Ensembl. Available at: https://www.ensembl.org/Homo_sapiens/Transcript/Summary?db=core;g=ENSG00000293464;r=14:62127244-62128537;t=ENST00000555934 [Last accessed on December 12, 2024]
20 Transcript: ENST00000415070.1. Ensembl. Available at: https://www.ensembl.org/Homo_sapiens/Transcript/Summary?db=core;g=ENSG00000228499;r=2:235882362-235882493;t=ENST00000415070 [Last accessed on December 12, 2024]
21 Transcript: ENST00000587701.1. Ensembl. Available at: https://www.ensembl.org/Homo_sapiens/Transcript/Summary?db=core;g=ENSG00000267139;r=19:3118665-3119304;t=ENST00000587701 [Last accessed on December 12, 2024]
22 Detail infomation of NONHSAT075167.2. NONCODE. Available at: http://v5.noncode.org/show_rna.php?id=NONHSAT075167&version=2&utd=1# [Last accessed on December 12, 2024]
23 Detail infomation of NONHSAT188126.1. NONCODE. Available at: http://v5.noncode.org/show_rna.php?id=NONHSAT188126&version=1&utd=1# [Last accessed on December 12, 2024]
24 Detail infomation of NONHSAT180080.1. NONCODE. Available at: http://v5.noncode.org/show_rna.php?id=NONHSAT180080&version=1&utd=1# [Last accessed on December 12, 2024]
25 Detail infomation of NONHSAT174445.1. NONCODE. Available at: http://v5.noncode.org/show_rna.php?id=NONHSAT174445&version=1&utd=1# [Last accessed on December 12, 2024]
26 ZFLNCG12153. BioChen.org. Available at: https://www.biochen.org/zflnc/ZFLNCG12153 [Last accessed on December 12, 2024]
27 ZFLNCG00215. BioChen.org. Available at: https://www.biochen.org/zflnc/ZFLNCG00215 [Last accessed on December 12, 2024]
28 ZFLNCG07732. BioChen.org. Available at: https://www.biochen.org/zflnc/ZFLNCG07732 [Last accessed on December 12, 2024]
29 Transcript: ENST00000405276.2. Ensembl. Available at: https://www.ensembl.org/Homo_sapiens/Transcript/Summary?db=core;g=ENSG00000217624;r=X:41675760-41676494;t=ENST00000405276 [Last accessed on December 12, 2024]
30 Lughmani H, Patel H, Chakravarti R: Structural features and physiological associations of human 14-3-3ζ pseudogenes. Genes (Basel) 15(4): 399, 2024. DOI: 10.3390/genes15040399
31 Lee H, Lim TS, Kim SU, Kim HC: Long-term cardiovascular outcomes differ across metabolic dysfunction-associated fatty liver disease subtypes among middle-aged population. Hepatol Int 16(6): 1308-1317, 2022. DOI: 10.1007/s12072-022-10407-7
32 Kang SH, Lee HW, Yoo JJ, Cho Y, Kim SU, Lee TH, Jang BK, Kim SG, Ahn SB, Kim H, Jun DW, Choi JI, Song DS, Kim W, Jeong SW, Kim MY, Koh H, Jeong S, Lee JW, Cho YK, Korean Association for the Study of the Liver (KASL): KASL clinical practice guidelines: Management of nonalcoholic fatty liver disease. Clin Mol Hepatol 27(3): 363-401, 2021. DOI: 10.3350/cmh.2021.0178
33 Kokkorakis M, Boutari C, Hill MA, Kotsis V, Loomba R, Sanyal AJ, Mantzoros CS: Resmetirom, the first approved drug for the management of metabolic dysfunction-associated steatohepatitis: Trials, opportunities, and challenges. Metabolism 154: 155835, 2024. DOI: 10.1016/j.metabol.2024.155835
34 Ma J, Yin H, Li M, Deng Y, Ahmad O, Qin G, He Q, Li J, Gao K, Zhu J, Wang B, Wu S, Wang T, Shang J: A comprehensive study of high cholesterol diet-induced larval zebrafish model: a short-time *in vivo* screening method for non-alcoholic fatty liver disease drugs. Int J Biol Sci 15(5): 973-983, 2019. DOI: 10.7150/ijbs.30013
35 Fam TK, Klymchenko AS, Collot M: Recent advances in fluorescent probes for lipid droplets. Materials (Basel) 11(9): 1768, 2018. DOI: 10.3390/ma11091768
36 Le TT, Ziemba A, Urasaki Y, Brotman S, Pizzorno G: Label-free evaluation of hepatic microvesicular steatosis with multimodal coherent anti-Stokes Raman scattering microscopy. PLoS One 7(11): e51092, 2012. DOI: 10.1371/journal.pone.0051092
37 Tripathi R, Chakraborty P, Varadwaj PK: Unraveling long non-coding RNAs through analysis of high-throughput RNA-sequencing data. Noncoding RNA Res 2(2): 111-118, 2017. DOI: 10.1016/j.ncrna.2017.06.003
38 ZFLNCG02400. BioChen.org. Available at: https://www.biochen.org/zflnc/ZFLNCG02400 [Last accessed on December 12, 2024]